



## 3D microdosimetric model to plan and control *in vitro* drug delivery mediated by nsPEFs with GCPW system

Laura Caramazza<sup>(1,2)</sup>, Alessandra Paffi<sup>(2)</sup>, Micaela Liberti<sup>(1,2)</sup>, and Francesca Apollonio<sup>(1,2)</sup>

(1) CLNS@Sapienza, Istituto Italiano di Tecnologia, Rome, Italy, 00161; corr. e-mail: laura.caramazza@iit.it

(2) DIET@Sapienza University of Rome, Italy, 00184; corr. e-mail: francesca.apollonio@uniroma1.it

### Abstract

Nanosecond pulsed electric fields (nsPEFs) with their wide frequency content, are recently known to be able to interact with cellular and subcellular membranes inducing reversible membrane permeabilization for biomedical applications. To improve treatments efficacy, lipid vesicles are studied and designed as smart delivery system able to respond to nsPEFs. In this work, authors report the study of an experimental bench suitable for *in vitro* exposure of cells and liposome nanocarriers to nsPEFs, compliant with the wideband requirements for nanosecond pulses. A multiphysics modelling able to predict cell and liposome nanoelectroporation is proposed to define the characteristics of signals to be used in experiments.

### 1 Introduction

Nanosecond pulsed electric fields (nsPEFs) with amplitude in the order of MV/m can interact with biological tissue, i.e. inducing the formation of aqueous pores on phospholipid bilayers that determines an increase of membrane permeability and the easily entry of therapeutic compounds, genetic materials and biomolecules inside the cell [1].

To both protect these molecules and reduce their toxicity with healthy tissue, stimuli-responsive nanocarriers, also called *smart drug delivery systems*, are studied as promising tools able to deliver the transported compounds in response to an internal or external trigger (such as pH, temperature, magnetic and electric fields) [2]. Among biocompatible lipid nanoparticles, liposomes, which are phospholipid vesicles composed by a bi-layered membrane like plasma membrane, are able to transport both hydrophobic and hydrophilic compounds, easily produced and targeted to achieve specific tissue [3].

In this context, a challenging aim is to use nsPEFs as actuators of drug delivery from liposomes, increasing liposome membrane permeability, and simultaneously providing the uptake inside the target cell of compounds across the plasma membrane. In the last years numerical studies obtained promising results investigating the feasibility to nanoelectroporate a solution of liposomes (with diameter ranging from 100 to 1000 nm) in absence [4] and presence of a cell as extracellular and/or intracellular particles [5,6].

Recently, the experimental feasibility to nanoelectroporate liposomes with nanosized dimension using a train of 10 ns-

duration pulses and intensities in the order of MV/m has been proven in [7] using standard electroporation parallel plate sample holder filled with liposomes solution.

Moreover, to overcome the known technological limits of the parallel plate system in terms of impedance matching and give the chance to expose a wide range of conductivity samples authors proposed in [8,9] a grounded coplanar waveguide (GCPW) system compatible with the use of nsPEFs.

Here authors provide the experimental characterization of the nsPEFs signal transmitted in the GCPW exposure setup for solutions of high conductivity. Moreover, through a sophisticated 3D microdosimetry both in frequency and time domain, they give the numerical feasibility to simultaneously nanoelectroporate cell and liposomes with the same electric field intensities as a starting point for setup *in vitro* drug delivery experiments.

### 2 Materials and Methods

#### 2.1 Experimental bench setup and nsPEFs signal characterization

The complete experimental setup to expose *in vitro* samples, is described in [9] and here briefly reported in Fig. 1-A: a ns pulser (FPG 10-1NM10, FID Technologies, Germany) is connected to port 1 of the GCPW through a high voltage coaxial cable and connectors. The port 2 of the GCPW is connected to a 50-Ω matching load. The experimental bench is completed with a couple of high voltage probes (TT-HVP 2739, Testec, Germany), able to detect the nsPEFs signal and connected to an oscilloscope (RTO2014, Rohde & Schwarz, Germany) to acquire the signal in time.

The nsPEFs generator delivers a sequence of pulses, characterized by: (i) 10 ns as duration at half maximum amplitude; (ii) rise/fall times of about 2 ns; (iii) intensities ranging from 2 to 10 kV; (iv) pulse repetition frequencies (PRF) from 1 to 1000 Hz. Here authors characterize the signal delivered by the generator connected to the oscilloscope through a series of four attenuators and setting the generator at 10 kV and PRF of 2 Hz.

The GCPW system here proposed is reported in detail in Fig. 1-B and has been previously fabricated as in [8] and described in [9]. Main dimensions of the structure are reported as follows: (i) 120 mm in total length; (ii) 50 mm in width; (iii) 1.524 mm in height; (iv) 2 mm in gap width.

The teflon sample holder for solutions, placed at 60 mm from the port 1, is 11 mm in diameter, 8 mm in height and 2 mm in wall thickness.

A set of measurements has been performed to characterize the nsPEFs signal in a saline solution sample, considered as a benchmark for future *in vitro* drug delivery experiments. Electrical conductivity of the saline solution is 1.4 S/m (evaluated as in [7]). Specifically, this conductivity is typical of *in vitro* experiments of studies on human mesenchymal stem cells (MSCs) [10,11].

## 2.2 Microdosimetric model

In order to provide the feasibility to nanoelectroporate both plasma membrane and liposome during nsPEFs exposure, 3D numerical simulations have been performed using the software COMSOL Multiphysics v 5.5. The 3D model shown is reported in Fig. 1-(C,D), with main dimensions as in Table 1. The extracellular medium is represented by a box with 70  $\mu\text{m}$  in height, like the electrodes thickness in the GCPW system [12], in which an ellipsoidal shaped cell is placed (Fig. 1-C) together with a group of 5 liposomes near the upper pole of the cell (Fig. 1-D). Cell size has been chosen referring to real MSCs cells [10,11].

Plasma and liposome membrane are set as boundary conditions. The front and back sides of the box are set to the ground and potential electrode, respectively.

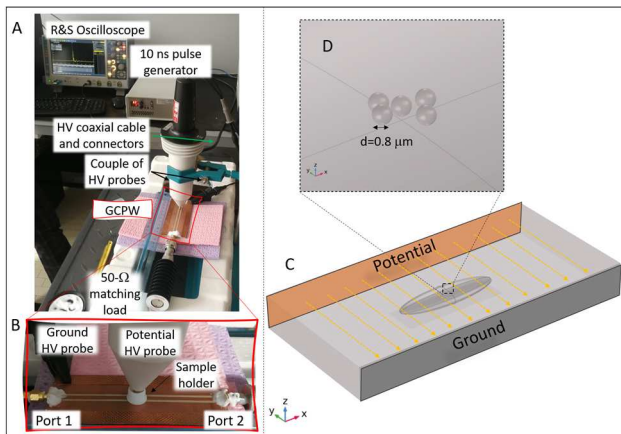


**Figure 1.** A) Experimental setup in place for nsPEFs characterization and exposures with GCPW system. B) Detail of the GCPW system with a sample holder and the two HV probes. C) 3D model of the extracellular medium surrounding cell and liposomes. D) Detail of the 5 liposomes randomly distributed near the cell.

Dielectric parameters, reported in Table 1, are set considering previous studies in literature [7,10,13]. Dielectric dispersion parameters have been set as in [13,14].

Spectral response of cell and liposomes has been studied from 1 kHz to 1 GHz, with E field=1 V/m, to confirm that above  $\beta$ -relaxation, within the frequency content of ultra-short pulses the two response are fully comparable.

The electromagnetic problem has been solved both in frequency and time domain using the Electric Currents mode of the AC/DC module in Comsol.

The application of a 10 ns-duration pulse on this model has been studied with E field intensities from 2 to 10 MV/m, in line with amplitudes used in literature [4,5,7,10]. The pore density kinetics has been evaluated using the asymptotic equation firstly proposed by De Bruin and Krassowska [15] for cell electropermeabilization.

**Table 1.** Material properties used in microdosimetric models.

Properties of materials	$\sigma$ [S/m]	$\epsilon_r$	Dimension [ $\mu\text{m}$ ]
Extracellular solution	1.4	67	Box 600x300x70
Plasma membrane	$1.1 \times 10^{-7}$	11.7	0.005
Cytoplasm	0.3	67	Ellipsoid: 210x60x25
Liposome membrane	$1.1 \times 10^{-7}$	11.7	0.005
Liposome inner solution	0.35	67	0.800

Pore density kinetics depends on the induced transmembrane potential (TMP) changes in time and determines the increase in membrane conductivity, reducing the insulating properties of the membrane. According to this model [7], membrane conductivity depends not only on pore density (N) values but also on TMP, temperature, pore conductivity and pore radius.

Therefore, in this work for the first time the evolution in time of pore radius has been investigated, considering the pores as a homogeneous population [16] and solving the time dependent equation as follows [17]:

$$\frac{dr}{dt} = \frac{D}{kT} \left\{ \frac{TMP^2 F_{max}}{1+r_h/(r+r_t)} + 4\beta \left( \frac{r_*}{r} \right)^4 \frac{1}{r} - 2\pi\gamma + 2\pi\gamma_{eff}r \right\} \quad (1)$$

where  $\gamma_{eff}$  is the effective surface tension and is described as follows:

$$\gamma_{eff} = 2\gamma' - \frac{2\gamma' - \gamma_0}{(1 - \pi N r^2)^2} \quad (2)$$

Pore density and pore radius kinetics have been solved using two Boundary ODEs and DAEs modes of Comsol for plasma and liposome membranes. All parameters have been set as in [17]. In literature the thresholds for achieving electroperoration are a TMP > 1 V and  $N > 10^{14} \text{ m}^{-2}$ .

## 3 Results

### 3.1 nsPEF exposure setup and signal characterization

Fig. 2-A shows the results of the signal delivered from the generator, reported as the average signal of a train of about 10 pulses  $\pm$  standard deviation showing a good agreement with a trapezoidal shape. Results of the signal measured inside the sample holder filled with 1.4 S/m solution sample are shown in Fig. 2-B as the normalized average signal of a train of about 20 pulses  $\pm$  standard deviation. Here, the signal almost preserves the 10 ns duration, even if the probe is in contact with the teflon holder. These results confirm the good broadband behaviour of the GCPW to be used as nsPEFs exposure system.

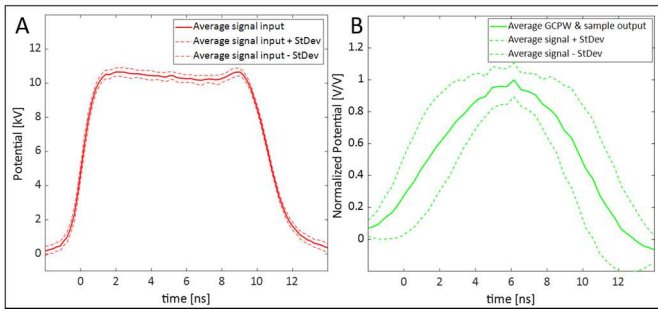


**Figure 2.** Average (solid curves)  $\pm$  standard deviation (dashed curves) of the signals delivered from the generator (A) and detected on the sample solution holder (B), respectively in red and green curves.

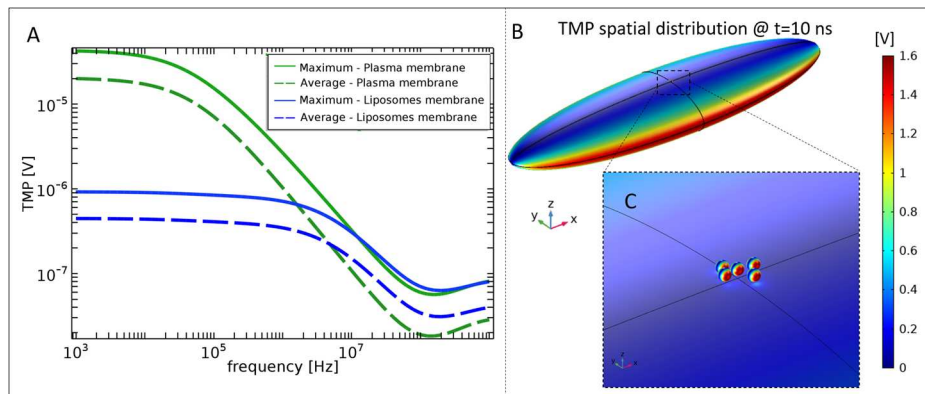
### 3.2 3D microdosimetric study results

The frequency analysis in the range ( $10^3$ - $10^9$  Hz) confirms the role of shape and dimensions of cell and liposomes. Fig. 3-A shows that for both cell and liposomes membranes the TMP maintains the typical low-pass filter behaviour [18] in terms of maximum and average values. The overall trend is in accordance with analytical results in literature [5], here the  $\beta$ -relaxation occurs at  $10^4$  Hz and  $10^6$  Hz respectively for cell and liposomes membranes. Considering the

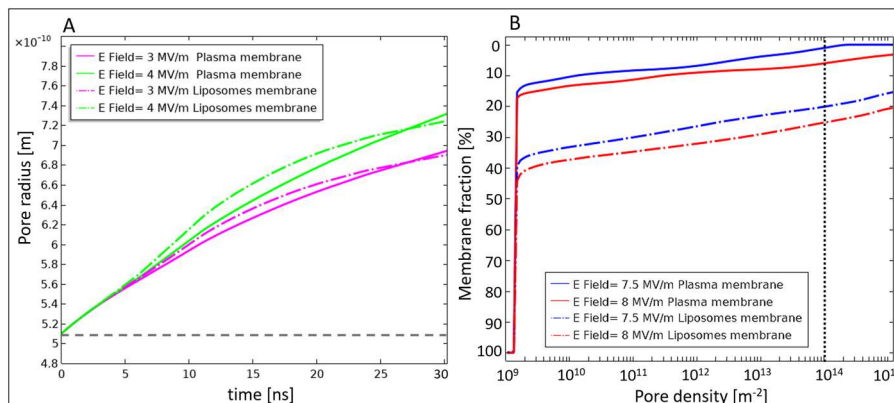
frequency content of 10 ns pulse, with the first lobe of about 100 MHz, the similar behaviour above  $\beta$ -relaxation is confirmed.

Fig. 3-B reports the spatial distribution of the TMP evaluated at the pulse plateau ( $t=10$  ns) for the cell, while Fig. 3-C for the liposomes. In line with [5], the TMP values overcoming the threshold for electroporation are located to the poles of both cell and liposomes facing the electrodes, while lower values are shown at the equators.

Fig. 4-A shows that the pore radius, starting from a value of 0.51 nm [17] for unperturbed membranes, strongly increases in time due to the 10 ns pulse application in both cell and liposome membranes, already for E field intensities of 3 and 4 MV/m. Applying higher E field values of 7.5 MV/m, we reach nanoporation of both cell and liposome membranes. In particular, Fig. 4-B shows that when pore density in cell membrane is about 2% (demonstrated to be a threshold for electroporation of cells [10]), a 20% of porated membrane is achieved for liposomes. Increasing E field amplitude up to 8 MV/m we obtained 10 % of poration for the cell and above 35 % for liposome. This is perfectly compatible with the planned experiments, where while we aim to strongly porate the liposomes to facilitate the release of their cargo, we need to moderately porate the cells to preserve their viability.



**Figure 3.** A) Induced TMP in frequency on cell (green curves) and liposome (blue curves) in terms of maximum and average values (solid and dashed curves respectively). B) TMP spatial distribution on cell and liposome membranes at  $t=10$  ns evaluated for E field= 7.5 MV/m. C) Detail of the TMP distribution on liposome membranes.



**Figure 4.** A) Pore radius evolution in time for plasma membrane and liposome membrane (solid and dashed/dotted curves respectively) applying 3 and 4 MV/m (magenta and green, respectively). B) Results of % of membrane fraction porated for cell and liposomes (solid and dashed/dotted curves respectively), for E field intensities of 7.5 and 8 MV/m.

## 4 Conclusion

An experimental bench for nsPEFs drug delivery application with a GCPW as exposure system has been presented and characterized when a train of 10 ns pulses at high intensities is applied. A 3D microdosimetric model has been built in order to evaluate the possibility to simultaneously nanoelectroporate cell and liposomes using a single 10 ns pulse.

The increase of pore radius on membranes has been detected for E field values starting from 3 MV/m. Time evolution of pore radius provides more information on the not yet deeply known mechanisms of electroporation and gives the chance to design *in vitro* drug delivery experiments with GCPW system and a train of nsPEFs.

## 5 Acknowledgements

F. A. acknowledges financial support from the Sapienza University of Rome, Research Projects, 2018 (No. RM118164282B735A) and thanks the COST Action CA15211— Atmospheric Electricity Network: coupling with the Earth System, climate and biological systems (Electronet). M. L. acknowledges financial support from the Sapienza University of Rome, Research Projects, 2017 (No. RM11715C7DCB8473).

## 6 References

- [1] T. Kotnik, L. Rems, M. Tarek, and D. Miklavčič, “Membrane Electroporation and Electroporabilization: Mechanisms and Models,” *Annu Rev Biophys*, vol. 48, 63-91, 2019.
- [2] S. Hossen, M. K. Hossain, M.K. Basher, M.N.H. Mia, M.T. Rahman, M.J. Uddin, “Smart nanocarrier-based drug delivery systems for cancer therapy and toxicity studies: a review”, *J Adv Research*, 15 (2019) 1-8.
- [3] S. Senapati, A. K. Mahanta, S. Kumar, and P. Maiti, “Controlled drug delivery vehicles for cancer treatment and their performance,” *Signal Transduct. Target. Ther.*, vol. 3, no. 1, p. 7, 2018.
- [4] A. Denzi, E. della Valle, G. Esposito, L. M. Mir, F. Apollonio, and M. Liberti, “Technological and Theoretical Aspects for Testing Electroporation on Liposomes,” *Hindawi BioMed Research International*, vol. 2017, article ID 5092704, 10 pages, March 2017.
- [5] A. Denzi, E. della Valle, F. Apollonio, M. Breton, L. M. Mir, and M. Liberti, “Exploring the Applicability of Nano-Poration for Remote Control in Smart Drug Delivery Systems,” *J Membr. Biol*, vol. 250, pp. 31-40, 2017.
- [6] L. Retelj, G. Pucihar, and D. Miklavcic, “Electroporation of Intracellular Liposomes Using Nanosecond Electric Pulses — A Theoretical Study,” *IEEE Trans Biomed Eng.*, vol. 60, issue 9, pp. 2624-2635, 2013.
- [7] Caramazza, L.; Nardoni, M.; De Angelis, A.; Paolicelli, P.; Liberti, M.; Apollonio F.; Petralito, S.: Proof-of-Concept of Electrical Activation of Liposome Nanocarriers: From Dry to Wet Experiments, *Front. Bioeng. Biotechnol.*, 8:819, 2020.
- [8] A. Paffi, A. Banin, A. Denzi, M. Casciola, M. Liberti, and F. Apollonio “Broadband coplanar system for in vitro experiments,” 2019 European Microwave Conference in Central Europe (EuMCE), Prague, Czech Republic, 2019, pp. 639-642.
- [9] L. Caramazza, A. Paffi, M. Liberti and F. Apollonio, "A Coplanar Waveguide System for Drug Delivery Mediated by Nanoelectroporation: an Experimental and Numerical Study," 2020 50th European Microwave Conference (EuMC), Utrecht, Netherlands, 2021, pp. 999-1002, doi: 10.23919/EuMC48046.2021.9338023.
- [10] De Angelis, A., Denzi, A., Merla, C., Andre, F. M., Mir, L. M., Apollonio, F., Liberti, M., & Romeo, S. (2020). Confocal Microscopy Improves 3D Microdosimetry Applied to Nanoporation Experiments Targeting Endoplasmic Reticulum. *8*, 1–9. doi: 10.3389/fbioe.2020.552261
- [11] Hanna, H., Denzi, A., Liberti, M., André, F. M., and Mir, L. M. (2017). Electroporabilization of inner and outer cell membranes with microsecond pulsed electric fields: quantitative study with calcium ions. *Sci. Rep.* 7:13079. doi: 10.1038/s41598-017-12960-w
- [12] M. Casciola, S. Xiao, F. Apollonio, A. Paffi, M. Liberti, C. Muratori, A. G. Pakhomov, “Cancellation of nerve excitation by the reversal of nanosecond stimulus polarity and its relevance to the gating time of sodium channels,” *Cell Mol Life Sci.*;76(22):4539-4550, 2019.
- [13] Denzi, A., Camera, F., Merla, C., Benassi, B., Consales, C., Paffi, A., Apollonio, F., & Liberti, M. (2016). A Microdosimetric Study of Electropulsation on Multiple Realistically Shaped Cells: Effect of Neighbours. *Journal of Membrane Biology*, 249(5), 691–701. doi: 10.1007/s00232-016-9912-3
- [14] Denzi A, Merla C, Camilleri P, Paffi A, d’Inzeo G, Apollonio F, Liberti M (2013) Microdosimetric study for nanosecond pulsed electric fields on a cell circuit model with nucleus. *J Membr Biol* 246:761–767.
- [15] K. A. DeBruin and W. Krassowska, “Modeling electroporation in a single cell. I. Effects of field strength and rest potential,” *Biophys. J.*, vol. 77, no. 3, pp. 1213–1224, 1999.
- [16] Neu, J. C., and W. Krassowska. "Modeling postshock evolution of large electropores." *Physical review E* 67.2 (2003): 021915.
- [17] Krassowska, W., and P. D. Filev. "Modeling electroporation in a single cell." *Biophysical journal* 92.2 (2007).
- [18] C. Polk, E. Postov, “Biological effects of electromagnetic fields.” *CRC handbook*, 2nd edn. CRC, Boca Raton, (1995).